Semiconductor Physics, Quantum Electronics & Optoelectronics, 2021. V. 24, No 2. P. 139-147.

Semiconductor physics

Properties of nanosized ZnO:Ho films deposited using explosive evaporation

A.M. Kasumov[1], V.V. Strelchuk[2], O.F. Kolomys[2], O.I. Bykov[1], V.O. Yukhymchuk[2], M.M. Zahornyi[1], K.A. Korotkov[1], V.M. Karavaieva[1], S.F. Korychev[1], A.I. Ievtushenko[1]

[1]I. Frantsevych Institute for Problems of Materials Science, NAS of Ukraine
3, Krzhyzhanivskoho str., 03142 Kyiv, Ukraine
E-mail: kasumov@ipms.kiev.ua
[2]V. Lashkaryov Institute of Semiconductor Physics, NAS of Ukraine,
41, prosp. Nauky, 03680 Kyiv, Ukraine
E-mail: viktor.strelchuk@ccu-semicond.net

Abstract. The properties of nanosized ZnO:Ho thin films deposited by explosive evaporation method have been studied. This work is aimed at studying the effect of high deposition rate on the oxide characteristics interesting from the viewpoint of photocatalysis, namely: morphology and structure, electrical and optical properties, lifetime of charge carriers. Explosive deposition of films defines the novelty of this work as compared to majority of previous studies devoted to nanosized ZnO:Ho photocatalysts, which used equilibrium methods for their synthesis. Methods of scanning electron microscopy, XRD analysis, photoluminescence, and Raman scattering have shown that in ZnO:Ho films deposited using explosive evaporation, with increasing holmium content, amorphization of their structure and morphology are observed. It is related with random incorporation of holmium atoms into the crystalline lattice of ZnO as well as with the fact that the ionic radius of Ho^{3+} exceeds that of Zn^{2+}. It is accompanied by a shift of the edge of ZnO absorption toward the long-wave (blue) spectral range, the decrease of the bandgap as well as an increase in the resistivity and lifetime of charge carriers. All these changes are favourable for the photocatalytic process involving nanostructures based on ZnO:Ho.

Keywords: zinc oxide film, holmium, photocatalyst, explosive evaporation.

https://doi.org/10.15407/spqeo24.02.139
PACS 61.05.cp, 68.37.Ef, 72.80.Ey, 78.20.-e, 78.30.Ly, 78.55.Qr

Manuscript received 16.02.21; revised version received 07.04.21; accepted for publication 02.06.21; published online 16.06.21.

1. Introduction

Zinc oxide ZnO, due to the successful combination of chemical inertness, transparency, bactericidal properties, relatively cheaper and easier production is widely used in paint-and-vanish, rubber, chemical, pharmaceutical, oil refining, glass, and electronic industries. In particular, doping of ZnO with the rare-earth metal holmium and other elements has shown that doped ZnO exhibits ferromagnetic [1, 2], ferroelectric [3], thermoelectric [4], photoluminescent [5–8], electroluminescent [9], and photocatalytic [10–13] properties, which are of undoubted interest for practical applications. The current studies allow revealing new properties of ZnO films doped with holmium.

Studies of this material have revealed that most of these properties largely depend on the size and shape of the crystals, their structure, impurity concentration, presence and nature of defects, as well as on other parameters related to manufacturing technology. The synthesis of ZnO:Ho is usually performed using such known methods as co-precipitation from solution [3, 14], sol-gel treatment [1, 5, 6, 15], sonochemical synthesis [10, 12], solid-state reactions [2, 4, 9, 13, 16, 17], thermal evaporation [18], which can be roughly attributed to equilibrium methods, which provide the time required for ascertaining the structure of the obtained material. At the same time, it is of interest to study the properties of ZnO:Ho films, which are caused by very rapid evaporation of the initial material. It is expected that the high deposition rate should positively affect the properties of nanosized films.

This work is aimed at studying the properties of nanosized ZnO:Ho films deposited on silica substrates by using the explosive evaporation mode in the electron-beam method of growing. The main attention was paid to the properties that are important for the process of photocatalysis, namely: morphology, structure, optical properties and lifetime of charge carriers.

2. Experimental

ZnO:Ho thin films were deposited on silica substrates by using explosive evaporation of a mixture of fine Zn and Ho powders taken in the required ratio. The mixture of powders was delivered to the region of evaporation triggered by an electron beam with the energy of electrons 6 keV and the flux density close to 1 A/cm^2 in the VU-1A vacuum setup. The obtained Zn:Ho films were annealed in air in a muffle furnace for 1 hour at 300 °C up to formation of ZnO:Ho films. The Ho content was 0, 1, 2, 3, 4, and 5 at.%.

The films were deposited under the following conditions: pressure in the operation chamber p = $5\cdot10^{-3}$ Pa, substrate temperature T_s = 40 °C, maximum film deposition rate V_{max} = 90 nm/min. After the oxidation procedure, the film thickness increased by 20%, reaching the average value close to 80 nm for ZnO:Ho films. The samples were cooled together with the muffle furnace without hardening.

Examination of sample morphology was performed using the scanning microscope MIRA3 TESCAN. The optical transmission spectrum was recorded using the StellaNet Minispectrometer SilverNova. The lifetime of charge carriers was determined by the frequency method [19]. XRD analysis was performed using an upgraded DRON-3M diffractometer with Cu-Kα radiation.

The Raman measurements were carried out in a quasi-backscattering geometry at room temperature using the Horiba Jobin-Yvon T64000 triple spectrometer with integrated micro-Raman setup – Olympus BX-41 microscope (objective ×50, aperture 0.90) equipped with a motorized XYZ stage and Peltier-cooled CCD detector. Samples were excited by Ar/Kr laser (488 nm). Photoluminescence (PL) of deposited ZnO films was excited using a He-Cd laser (325 nm).

3. Results and discussion

3.1. Morphology of films

Undoped ZnO films deposited using explosive evaporation of Zn and oxidized by annealing at 300 °C consisted of crystals, the longest of which had the shape of rods with the average length of 125 nm and the width of 23 nm (Fig. 1a). The smallest crystals were globular with the diameter 17 nm. Medium-sized crystals had an intermediate ellipsoid shape.

The rod-like shape of large crystals may be, to some extent, a consequence of the hexagonal structure of ZnO. The curved shape of the rods indicates presence of structural defects caused by non-equilibrium growth conditions.

As the Ho content in ZnO films increases, the length of the rods decreases, and the thickness increases. This brings the crystals closer to a spherical shape. In this case, the volume of crystals increases with increasing Ho content by the parabolic law, due to its relation with the increasing rod diameter by a quadratic function (Fig. 2).

3.2. The structure of films

XRD analysis of films obtained from pure zinc allows us to conclude that in this case ZnO with a hexagonal structure is formed (Fig. 3). A significant difference between the obtained diffraction pattern and the standard one consists in the change in the intensity distribution of the diffraction peaks. The standard series of relative intensities I(100), I(002), I(101) for the ZnO structure, coinciding with the peak gravity centers, is recorded as 569:415:999. Our experiment demonstrates this series as 403:999:843. As seen, the change in the ratio of the peak intensities I(100)/I(101) does not exceed 10% compared to the standard, and the relative intensity (002) is 100%.

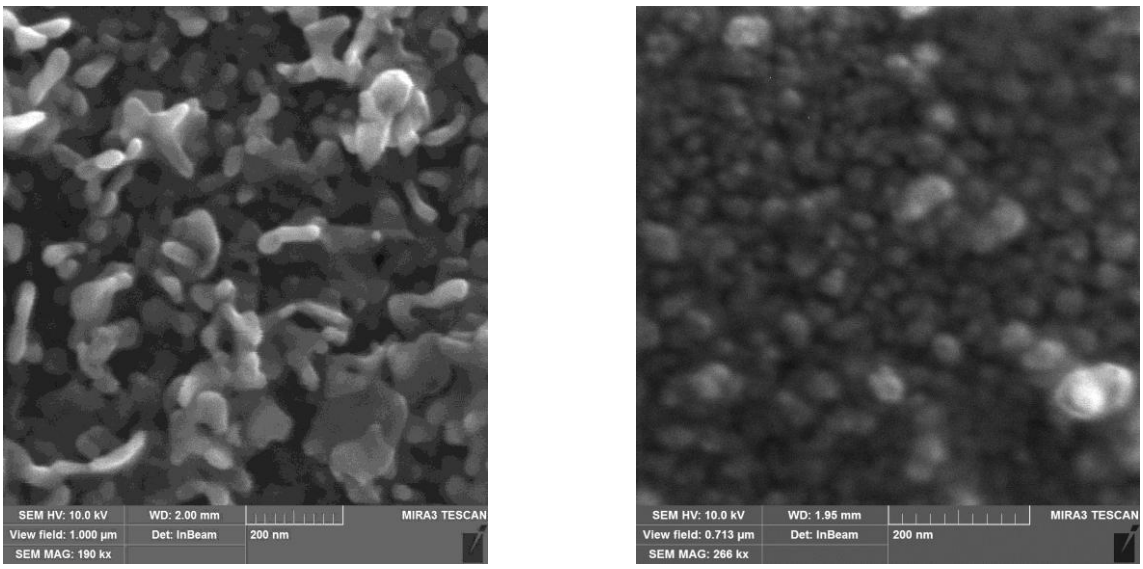

a) b)

Fig. 1. Morphology of ZnO:Ho films with holmium content of 0 (a) and 5 (b) at.%.

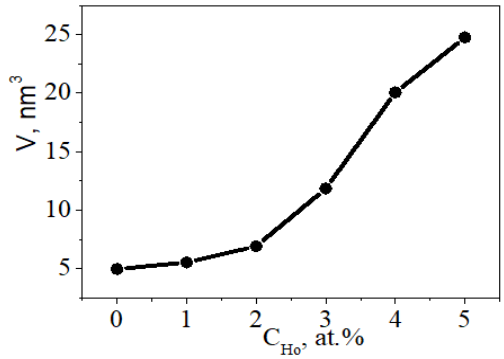

Fig. 2. Dependence of the volume *V* of the largest crystals in ZnO:Ho films on the holmium content C_{Ho}.

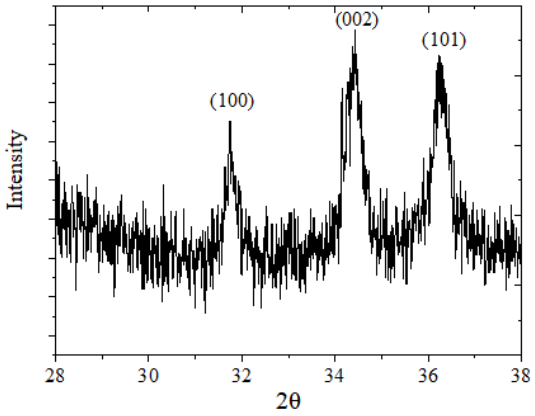

Fig. 3. Fragments of XRD pattern from ZnO film.

This effect can be attributed to formation of a film with the initial orientation of the (002) plane of crystallites (coherent scattering region) relative to the silica substrate plane.

The size of crystallites was calculated using the Scherer formula:

$$D = \frac{0.9\lambda}{W\cos\theta}, \qquad (1)$$

where *D* is the crystallite size, *W* – broadening of the line, θ – Bragg angle, λ – wavelength of X-ray radiation.

The sizes of crystallites calculated according to this formula in the direction of the c-axis in the crystal lattice are close to 20.6 nm, and in the perpendicular direction – 27.6 nm. Oxidation of coatings containing holmium leads to formation of ZnO films with low crystallinity. The intensity of the diffraction peaks (100), (002), and (101) decreases, and their broadening increases, which indicates, in the general case, changes in the crystallite sizes. With increasing the Ho content, the crystallite size decreases. In the region of Ho content 2…3%, the dimensions along the *c*-axis are about 12 nm, and in the base plane – up to 19 nm. In the Ho content range of 4 to 5%, these dimensions are close to 10…13 nm. This indicates that the shape of the crystallites is preserved, but the size ratio oscillates around 0.7 (Fig. 4).

The nature of the obtained dependences for the change in the crystallite size may be interpreted in terms of a decrease in the growth rate of ZnO nuclei with increasing content of holmium. The growth of nuclei of zinc oxide-based solid solution is hampered by differences in ion sizes and valences of the metals.

When holmium is introduced, the crystal lattice parameters and the volume of the unit cell change as well. It should be noted that, as known, the holmium ion Ho^{3+} radius is larger than that of Zn^{2+} by about 6% [20]. In the case of replacement of zinc atoms by holmium atoms or the latter entry into the interstitial sites of the ZnO crystal lattice, one can expect an increase in the zinc oxide lattice parameters. The results of calculations of lattice parameters *a*, *c*, and its volume showed some increase with increasing the Ho content.

At the Ho content within 0 to 2 at.%, the parameters *a* and *c* do not exceed 3.2521 and 5.2152 Å, respectively. The volume of the unit cell does not exceed 47.766 $Å^3$. With further increasing the Ho content, these parameters increase: the parameter *a* approaches to 3.258 Å, *c* does 5.22 Å. This is reflected in the volume change, which increases up to 48 $Å^3$ (Fig. 5).

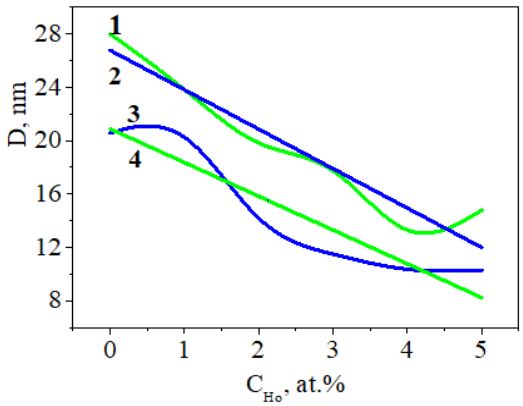

Fig. 4. Dependence of crystallite sizes of Ho doped ZnO on the Ho content: *1*, *3* – in the direction of *a*- and *c*-axes of the crystalline lattice respectively, smoothed by β-splines; *2*, *4* – approximation lines.

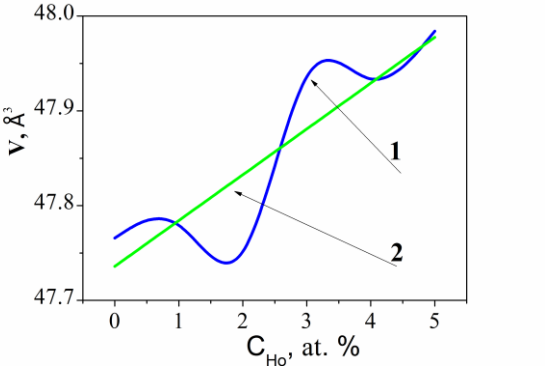

Fig. 5. Dependence of the crystal lattice volume on the Ho content: *1* – dependence smoothed by β-spline; *2* – approximation line.

Thus, we can assume that holmium ions are embedded into the ZnO crystal lattice. Herein, with increasing content of doping metal, as mentioned above, there is observed amorphization of the film material: the intensity of the diffraction peaks decreases, and their blurring increases, which is due to the reduction in the crystallite sizes.

3.3. Electrical properties and lifetime of charge carriers

The resistivity of undoped ZnO films is 500 Ohm·m, which is lower than that of bulk samples for this oxide [21]. The lower resistance is probably a consequence of their defective structure, which leads to the corresponding distortion of the crystal morphology (see, please, Fig. 1a).

With increasing the Ho content from 0 up to 5 at.%, the resistivity increases (Fig. 6).

On the one hand, this may be a result of weakening the contacts between the crystals, which takes place with increasing their volume. However, a more probable reason is the capture of charge carriers by traps, which here may be holmium atoms. This explains the linear increase in the resistivity ρ depending on the Ho content in ZnO.

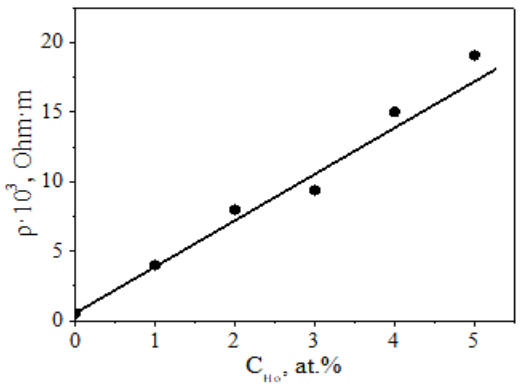

Fig. 6. Dependence of the resistivity ρ of ZnO:Ho films on the holmium content C_{Ho}.

The ρ (C_{Ho}) dependence increase is also noticeable in the images of the surface of ZnO:Ho films obtained using a scanning microscope (see Fig. 1). As shown, with increasing C_{Ho} the sharpness of the images deteriorates under the same conditions. This indicates that the electrons introduced into the films by electron beam are increasingly captured by the traps, creating a scattering field for the secondary and reflected electrons involved in creating the surface image.

The increase in the number of charge carrier traps, which is observed with increasing C_{Ho}, affects the lifetime of the carriers. The lifetime of charge carriers was determined using the frequency method in accord with the formula [19]:

$$\frac{I(\omega t)}{I(0)} = \frac{1}{\sqrt{I + \omega^2 \tau_n^2}}, \qquad (2)$$

where $I(\omega t)$ and $I(0)$ are amplitudes of the variable component of the photocurrent in the sample at the modulation frequency ω and $\omega \to 0$, respectively; τ_n is the lifetime of charge carriers.

Fig. 7 shows that, with increasing C_{Ho}, the lifetime of electrons τ_n increases almost linearly due to their presence in traps.

3.4. Optical properties

The bandgap width E_g of ZnO:Ho films was determined using the formula corresponding to the direct transitions between the valence and conduction bands in zinc oxide [22]:

$$\alpha = B\left(h\nu - E_g\right)^{1/2}, \qquad (3)$$

where α is the absorption coefficient, B – constant, $h\nu$ – energy of light quantum.

The evaluation according to this formula showed that with increasing C_{Ho} from 0 to 5 at.%, the bandgap E_g decreases from 3.2 to 3.1 eV (Fig. 8). *I.e.*, when C_{Ho} grows from 0 to 5 at.%, the absorption edge is shifted from λ = 388 nm toward the blue spectral range up to λ = 400 nm.

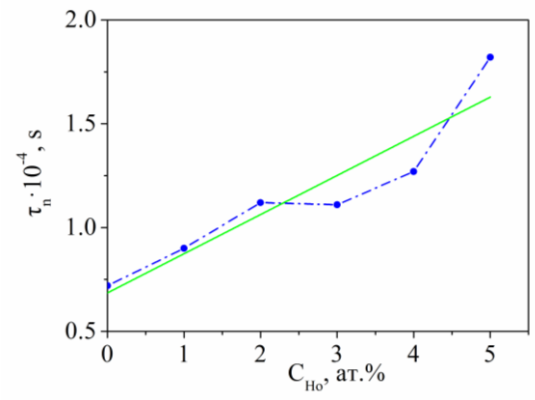

Fig. 7. Dependence of the lifetime of charge carriers τ_n on the Ho content C_{Ho} in ZnO:Ho films.

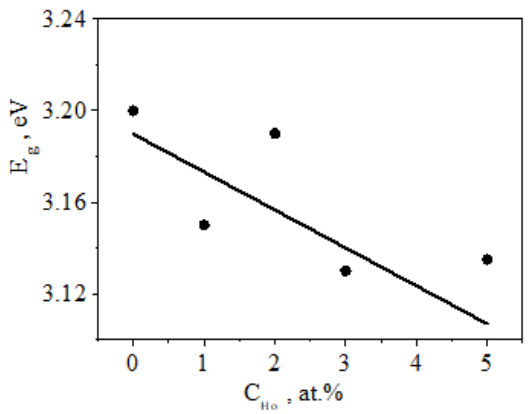

Fig. 8. Dependence of the optical width of forbidden band E_g of ZnO:Ho films on the Ho content C_{Ho}.

The decrease in E_g can also be associated with increasing the number of Ho ions randomly introduced using explosive sputtering into the ZnO structure, *i.e.*, with amorphization of films and increase in C_{Ho}. This amorphization leads to blurring of the edges of the band-gap E_g caused by the defect levels and to the corresponding decrease in the gap width.

3.5. Photoluminescence studies

The effect of doping ZnO films with Ho^{3+} ions on the edge, impurity, and intra-center optical radiation were studied using the photoluminescence method. Fig. 9 shows the room temperature photoluminescence spectra of undoped and 3 at.% Ho-doped ZnO thin films. In the PL spectra of both samples, there are intense bands of radiation in both the ultraviolet and visible ranges of the spectrum.

In the edge photoluminescence spectrum of the undoped ZnO film (curve *1*) in case of interband excitation (E_{exc} = 3.81 eV), there is an intense short-wave radiation band with the maximum at ~ 377.4 nm and half-width of approximately 12 meV, which is caused by radiative recombination of free excitons [23]. The shape of this photoluminescence band is characterized by a low-energy asymmetry and is modeled by three Gaussian contours with the peaks at 377.4, 385.6 and 394.2 nm and the distance that is multiple to the longitudinal optical (LO) phonon energy in ZnO crystal (~ 73 meV), which indicates the efficiency of radiative recombination processes with participation of LO phonons. The difference in the positions of the edge band maxima of ZnO films, as compared to that in bulk ZnO (368 nm) [24], is due to the presence of elastic deformations caused by mismatch of lattice parameters and coefficients of thermal expansion of the film and substrate [25].

The broad band peaking at 539 nm and the high-frequency wing at 605 nm are associated with radiative recombination processes that occur at deep energy levels in the bandgap and are caused by various types of intrinsic defects, such as ionized oxygen vacancies V_O and interstitial oxygen atoms O_i [26, 27].

In the photoluminescence spectra of Ho-doped ZnO thin films, a significant decrease in the intensity of the edge radiation band (by 6.5 times) and an increase in the intensity of the defect band are observed. The ratio of radiation intensity of the edges of the ultraviolet luminescence to that of defect luminescence (an optical indicator of structure quality) varies from 1.77 to 0.32, which indicates a significant increase in the number of intrinsic and impurity-caused structural defects with holmium doping [28]. In this case, XRD analysis showed (Fig. 4) a decrease in the size of the coherent scattering regions in ZnO, which leads to increasing the surface fraction and, accordingly, an increase in the concentration of surface centers of nonradiative recombination [29]. Also, the edge photoluminescence band of ZnO:Ho^{3+} significantly expands (G = 18 meV) from the low-energy side. This broadening in comparison with that in undoped ZnO films is probably caused by the

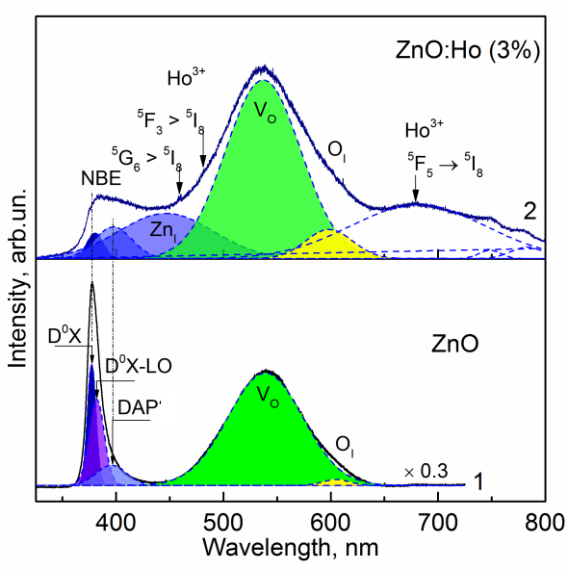

Fig. 9. Room temperature photoluminescence spectra of undoped (*1*) and Ho^{3+}-doped (*2*) ZnO thin films grown on silica substrates by electron-beam evaporation method. E_{exc} = 3.81 eV. T = 300 °C.

processes of elastic scattering of free (localized) excitons by potential fluctuations, intrinsic defects, and Ho^{3+} impurity centers. The shift of the edge radiation band from 377 to 380 nm upon doping with Ho^{3+} ions is related with presence of elastic tensile strains and variation of particle sizes. A larger ionic radius of Ho^{3+} (0.89 Å) as compared to that of Zn^{2+} ions (0.83 Å) [20] leads to significant distortion in the crystal structure of ZnO, which increases the concentration of defects in this material and, thus, the level of elastic strains. This band is well modeled considering two Gaussian bands with the peaks at 380 and 397 nm. The low-energy band at 397 nm may be related to radiative transitions of interstitial zinc atoms (Zn_i), which create a donor level below the conduction band by 0.22 eV [30], from which electrons are subsequently injected through the conduction band to the level of oxygen vacancies V_O [31]. The broad band at 446 nm, which is absent in the undoped ZnO film is associated with Zn_i as well, and its presence is determined by the growth conditions and thermal annealing (enrichment with Zn) [32].

Besides, the small bands at ~ 454 and 482 nm are observed in the photoluminescence spectra of the ZnO:Ho^{3+} film, which correspond to the intra-center electronic transitions of the Ho^{3+} center $^5G_6 \rightarrow {}^5I_8$ and $^5F_3 \rightarrow {}^5I_8$, respectively. The broad structureless band at 640…750 nm with a maximum at 680 nm and the band 740…760 nm can be associated with $^5F_5 \rightarrow {}^5I_8$ and $(^5F_5, {}^5S_2) \rightarrow {}^5I_7$ intra-center transitions, respectively; they can be markedly broaden due to significant inhomogeneity of the crystal field and high temperature [33]. Therefore, the appearance of additional radiation bands, which are absent in undoped ZnO films, confirms incorporation of Ho atoms into the ZnO lattice and replacement of Zn^{2+} ions by Ho^{3+} to some extent. The low intensity of the radiation bands associated with Ho^{3+}

ions may be caused by the inefficiency of the excitation energy (325 nm). This issue requires further low-temperature studies.

3.6. Raman scattering spectroscopy

The method of combinational scattering of light, the so-called Raman scattering, allows one to gain information about structural perfection, internal elastic deformations, degree of homogeneity by component composition and other properties of ZnO films and nanostructures. According to the theoretical group analysis, optical phonons of ZnO are described by irreducible representations in the Brillouin zone center: $G_{opt} = A_1 + 2B_1 + E_1 + 2E_2$ [34]. Polar A_1 and E_1 phonon vibrations are split into longitudinal optical (LO) and transverse optical (TO) phonon modes, which are manifested in the Raman spectra and infrared (IR) spectra. Inelastic scattering by E_2^{High} and E_2^{Low} phonon vibrations is permitted in the Raman spectra while scattering by B_1 symmetry vibrations (silent modes) is forbidden and does not manifest itself in the optical spectra of structurally perfect crystals. Fig. 10 demonstrates the Raman spectra of undoped and Ho-doped ZnO films. The spectrum of the undoped film contains well-known low-intensity E_2^{Low} and E_2^{High} phonon bands at ~ 99.5 cm^{-1} and 438.8 cm^{-1} (G ~ 13.0 cm^{-1}), respectively [35]. The frequency of E_2^{High} phonons of the ZnO film is shifted toward higher values by ~ 1.8 cm^{-1} as compared to that in the bulk ZnO crystal (437.0 cm^{-1}), which corresponds to the elastic compressive stresses in the film growth plane because of the mismatch of lattice parameters of the film and the substrate. The low intensity of all vibration bands indicates a low structural quality of the undoped oxide film.

After holmium incorporation into the ZnO lattice, the Raman spectrum of the ZnO:Ho^{3+} film undergoes a number of changes, which is primarily due to the effects of disordering the crystal structure. Phonons E_2^{Low} and E_2^{High} correspond to the vibrations of zinc and oxygen atoms in the cationic and anionic sublattices of wurtzite ZnO in the plane perpendicular to the *c*-axis and, accordingly, are sensitive to the disorder of the crystal structure of ZnO [36]. Doping the zinc oxide with holmium leads to broadening and low-frequency displacement of the E_2^{High} band maximum by ~ 4.0 cm^{-1} relatively to the frequency of undoped ZnO film due to significant tensile deformations (Fig. 10). This significantly increases the intensity of the asymmetric wing at the high-frequency side of E_2^{Low} band. The wing consists of two broad bands with the maxima at 115 and 137 cm^{-1} and is caused by transverse acoustic (TA) phonons around the M and K points of the Brillouin zone. Numerous internal and surface defects, in line with the presence of the dopant, break the translation symmetry of the crystal, which leads to the violation of the conservation law for wave vectors and participation of phonons with wave vectors $\vec{q} \neq 0$ in the Raman scattering.

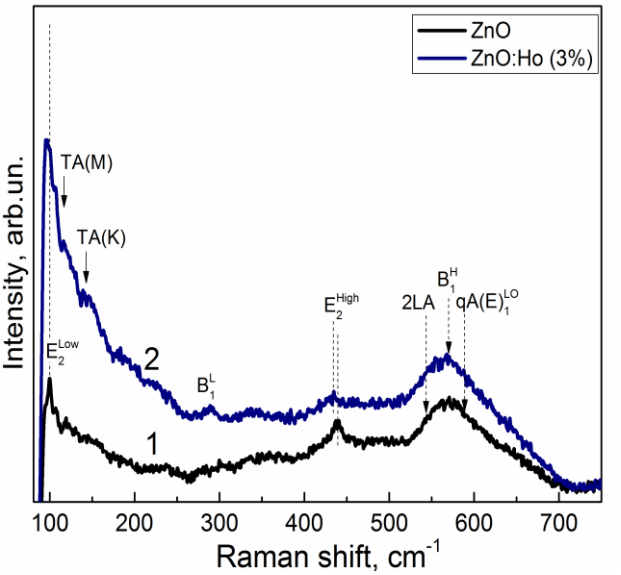

Fig. 10. Raman spectra of undoped (*1*) and Ho^{3+}-doped (*2*) ZnO thin films grown on quartz substrates by electron-beam evaporation method.

Moreover, in the Raman spectra of undoped and Ho-doped ZnO films, there is an additional broad band with a complex structure in the frequency range of 500 to 700 cm^{-1}. The increase in its intensity with holmium doping indicates its relation with addition of holmium or with an increase in the concentration of structural defects generated by this doping. The shape and position of this band is the result of the sum of several bands: i) band at 540 cm^{-1}, which is due to scattering by 2LA (H) phonons; ii) high-frequency band at 580 cm^{-1}, related to longitudinal E_1 (LO) phonons, and its position is determined by the superposition of scattering processes by A1 (LO) phonons at 574 cm^{-1} and E_1 (LO) phonons at 586 cm^{-1}; iii) band at ~ 550 cm^{-1} may also correspond to the silent B_1^H mode forbidden by the selection rules [35]. In addition, in the Raman spectrum of Ho-doped ZnO film, a band is observed at 288 cm^{-1}, which may correspond to the B_1^L ZnO mode. The high level of impurities or structural defects leads to weakening the selection rules for Raman scattering, and registration of this "forbidden" band becomes possible.

Hence, these studies have shown that the addition of Ho atoms to the ZnO matrix leads to structural disorder of the crystalline lattice and the appearance of additional scattering bands.

4. Conclusions

The obtained results show that in ZnO:Ho (0 to 5 at.%) thin films, deposited on silica substrates by using the electron-beam explosive evaporation method for growing, amorphization of their structure and changes in morphology are observed with increasing the holmium content, which is associated with the random incorporation of Ho atoms into the oxide crystal lattice. It is accompanied by decreasing the crystallite sizes from

20…27 down to 10…13 nm, shift of the absorption ZnO edge toward the blue spectral range from 388 up to 400 nm, decrease in the bandgap from 3.2 to 3.1 eV, increase in the resistivity from $5 \cdot 10^2$ up to $1.9 \cdot 10^6$ Ohm·m, increase in the lifetime of charge carriers from $7 \cdot 10^{-5}$ to $18 \cdot 10^{-5}$ s. All these changes are known to be favorable for the process of photocatalysis involving nanostructures based on ZnO, and may be the basis for further research in this area.

Acknowledgements

This work was supported by the research projects of NAS of Ukraine "Development of innovative photocatalytic nanostructured materials based on ZnO and TiO_2" (528/IPM-11/20).

References

1. Kabongo G.L., Mbule P.S., Mhlongo G.H. *et al.* Photoluminescence quenching and enhanced optical conductivity of P3HT-derived Ho^{3+}-doped ZnO nanostructures. *Nanoscale Res. Lett.* 2016. **11**. Article number 418. https://doi.org/10.1186/s11671-016-1630-3.
2. Akyol M., Ekicibil A., Kiymaç K. DC magnetic properties of the Ho doped ZnO compounds. *J. Supercond. Nov. Magn*. 2013. **26**. P. 3257–3262. https://doi.org/10.1007/s10948-013-2135-2.
3. Goel S., Sinha N., Kumar B. 3D hierarchical Ho-doped ZnO micro-flowers assembled with nanosheets: A high temperature ferroelectric material. *Physica E: Low-dimensional Systems and Nanostructures.* 2019. **105**. P. 29–40. https://doi.org/10.1016/j.physe.2018.09.002.
4. Pradyumnan P.P., Paulson A., Sabeer N.A.M., Deepthy N. Enhanced power factor in Ho^{3+} doped ZnO: A new material for TE application. *AIP Conf. Proc.* 2017. **1832**. P. 110055. https://doi.org/10.1063/1.4980679.
5. Mereu R.A., Mesaros A., Vasilescu M. *et al.* Synthesis and characterization of un-doped, Al and/or Ho doped ZnO thin films. *Ceramics Intern.* 2013. **39**, No 5. P. 5535–5543. https://doi.org/10.1016/j.ceramint.2012.12.067.
6. Singh S., Deepthi J.N.D., Ramachandran B., Rao M.S.R. Synthesis and comparative study of Ho and Y doped ZnO nano-particles. *Mater. Lett.* 2011. **65**. P. 2930–2933. https://doi.org/10.1016/j.matlet.2011.06.006.
7. Lashkarev G.V., Shtepliuk I.I., Ievtushenko A.I. *et al.* Properties of solid solutions, doped film, and nanocomposite structures based on zinc oxide. *Low Temperature Physics.* 2015. **41**. P. 129–144. https://doi.org/10.1063/1.4908204.
8. Ievtushenko A., Karpyna V., Eriksson J. *et al.* Effect of Ag doping on the structural, electrical and optical properties of ZnO grown by MOCVD at different substrate temperatures. *Superlattices and Microstructures.* 2018. **117**. P. 121–131. https://doi.org/10.1016/j.spmi.2018.03.029.
9. Ronfard-Haret J.-C., Azuma K., Bachir S., Kouyaté D., Kossanyi J. Electroluminescence of Ho^{3+} ions in semiconducting polycrystalline zinc oxide electrodes in contact with aqueous electrolyte. *J. Mater. Chem*. 1994. **4**, No 1. P. 139–144. https://doi.org/10.1039/JM9940400139.
10. Sheydaei M., Fattahi M., Ghalamchi L., Vatanpour V. Systematic comparison of sono-synthesized Ce-, La- and Ho-doped ZnO nanoparticles and using the optimum catalyst in a visible light assisted continuous sono-photocatalytic membrane reactor. *Ultrasonics Sonochem.* 2019. **56**. P. 361–371. https://doi.org/10.1016/j.ultsonch.2019.04.031.
11. Pant H.R., Pant B., Sharma R.K. *et al.* Antibacterial and photocatalytic properties of $Ag/TiO_2/ZnO$ nano-flowers prepared by facile one-pot hydrothermal process. *Ceramics Intern.* 2013. **39**, No 2. P. 1503–1510. https://doi.org/10.1016/j.ceramint.2012.07.097.
12. Phuruangrat A., Yayapao O., Thongtem T., Thongtem S. Preparation, characterization and photo-catalytic properties of Ho doped ZnO nanostructures synthesized by sonochemical method. *Superlattices and Microstructures.* 2014. **67**. P. 118–126. https://doi.org/10.1016/j.spmi.2013.12.023.
13. Hakimyfard A. and Mohammadi S. $ZnFe_2O_4$ and $ZnO\text{-}Zn_{1-x}M_xFe_2O_{4+\delta}$ (M = Sm^{3+}, Eu^{3+} and Ho^{3+}): Synthesis, physical properties and high performance visible light induced photocatalytic degradation of malachite green. *Adv. Powder Technol.* 2019. **30**, No 6. P. 1257–1268. https://doi.org/10.1016/j.apt.2019.04.005.
14. Ökte A.N. Characterization and photocatalytic activity of Ln (La, Eu, Gd, Dy and Ho) loaded ZnO nanocatalysts. *Appl. Catalysis A: General*. 2014. **475**. P. 27–39. https://doi.org/10.1016/j.apcata.2014.01.019.
15. Popa M., Schmerber G., Toloman D. *et al.* Magnetic and electrical properties of undoped and holmium doped ZnO thin films grown by sol-gel method. *Adv. Eng. Forum.* 2013. **8–9**. P. 301–308. https://doi.org/10.4028/www.scientific.net/AEF.8-9.301.
16. Franco A., Pessoni H.V.S. Optical band-gap and dielectric behavior in Ho-doped ZnO nanoparticles. *Mater. Lett.* 2016. **180**. P. 305–308. https://doi.org/10.1016/j.matlet.2016.04.170.
17. Sobczyk M., Marek Ł. Comparative study of optical properties of Ho^{3+}-doped $RE_2O_3\text{-}Na_2O\text{-}ZnO\text{-}TeO_2$ glasses. *J. Lumin.* 2019. **206**. P. 308–318. https://doi.org/10.1016/j.jlumin.2018.10.071.
18. Rai G.M., Iqbal M.A., Xu Y., Will I.G., Zhang W. Influence of rare earth Ho^{3+} doping on structural, microstructure and magnetic properties of ZnO bulk and thin film systems. *Chin. J. Chem. Phys*. 2011. **24**, No 3. P. 353–357. https://doi.org/10.1088/1674-0068/24/03/353-357.
19. Pavlov L.P. *Methods for Measuring the Parameters of Semiconductor Devices*. Vysshaya Shkola, Moscow, 1987 (in Russian).
20. Emsley J. *The Elements.* Oxford, Clarendon Press, 1991.

21. Samsonov G.V. *Physical and Chemical Properties of Oxides*. Moscow, Metallurgiya, 1978 (in Russian).
22. Pankove J. *Optical Processes in Semiconductors*. David Sarnoff Research Center, RCA Laboratories, New Jersey, 1971.
23. Chen Y.W., Liu Y.C., Lu S.X. *et al.* Optical properties of ZnO and ZnO:In nanorods assembled by sol-gel method. *J. Chem. Phys*. 2005. **123**. P. 134701. https://doi.org/10.1063/1.2009731.
24. Meyer B.K., Alves H., Hofmann D.M. *et al.* Bound exciton and donor-acceptor pair recombinations in ZnO. *phys. status solidi* (*d*). 2004. **241**, No 2. P. 231–260. https://doi.org/10.1002/pssb.200301962.
25. Singh J., Ranwa S., Akhtar J., Kumar M. Growth of residual stress-free ZnO films on SiO_2/Si substrate at room temperature for MEMS devices. *AIP Adv*. 2015. **5**. P. 067140. https://doi.org/10.1063/1.4922911.
26. Leiter F., Alves H., Pfisterer D. *et al.* Oxygen vacancies in ZnO. *Physica B: Condens. Matter.* 2003. **340–342**. P. 201–204. https://doi.org/10.1016/j.physb.2003.09.031.
27. Galdámez-Martinez, Santana G., Güell F. *et al.* Photoluminescence of ZnO nanowires: A review. *Nanomaterials.* 2020. **10**, No 5. P. 857. https://doi.org/10.3390/nano10050857.
28. Dixit T., Palani I.A. and Singh V. Selective tuning of enhancement in near band edge emission in hydrothermally grown ZnO nanorods coated with gold. *J. Lumin.* 2016. **170**. P. 180–186. https://doi.org/10.1016/j.jlumin.2015.10.003.
29. Matsumoto T., Kato H., Miyamoto K. *et al.* Correlation between grain size and optical properties in zinc oxide thin films. *Appl. Phys. Lett.* 2002. **81**. P. 1231. https://doi.org/10.1063/1.1499991.
30. Kayaci F., Vempati S., Donmez I. *et al.* Role of zinc interstitials and oxygen vacancies of ZnO in photocatalysis: A bottom-up approach to control defect density. *Nanoscale.* 2014. **6**. P. 10224–10234. https://doi.org/10.1039/C4NR01887G.
31. Cao B., Cai W., Zeng H. Temperature-dependent shifts of three emission bands for ZnO nanoneedle arrays. *Appl. Phys. Lett*. 2006. **88**. P. 161101. https://doi.org/10.1063/1.2195694.
32. Quemener V., Vines L., Monakhov E.V., Svensson B.G. Evolution of deep electronic states in ZnO during heat treatment in oxygen- and zinc-rich ambients. *Appl. Phys. Lett.* 2012. **100**, No 11. P. 112108. https://doi.org/10.1063/1.3693612.
33. Boyer J.C., Vetrone F., Capobianco J.A. *et al.* Optical transitions and upconversion properties of Ho^{3+} doped ZnO-TeO_2 glass. *J. Appl. Phys.* 2003. **93**, No 12. P. 9460–9465. https://doi.org/10.1063/1.1577817.
34. Damen T.C., Porto S.P.S., Tell B. Raman effect in zinc oxide. *Phys. Rev*. 1966. **142**. P. 570. https://doi.org/10.1103/PhysRev.142.570.
35. Manjon F.J., Mari B., Serrano J., Romero A.H. Silent Raman modes in zinc oxide and related nitrides. *J. Appl. Phys*. 2005. **97**. P. 053516. https://doi.org/10.1063/1.1856222.
36. Karpyna V., Ievtushenko A., Kolomys O. *et al.* Raman and photoluminescence study of Al, N-codoped ZnO films deposited at oxygen-rich conditions by magnetron sputtering. *phys. status solidi* (*d*). 2020. **257**, No 6. P. 1900788. https://doi.org/10.1002/pssb.201900788.

Authors and CV

Anatoliy M. Kasumov, PhD in Physics and Mathematics, Senior Researcher at the I. Frantsevych Institute for Problems of Materials Science, NAS of Ukraine. Author of more than 100 publications. His research interests include physics properties and technology of thin films.

Viktor V. Strelchuk, Professor, Doctor of Sciences in Physics and Mathematics, Head of Optical Submicron Spectroscopy Laboratory at the V. Lashkaryov Institute of Semiconductor Physics. Field of research: physics of semiconductors, Raman and photoluminescence spectroscopy of semiconductors, nanostructures and nanoscale materials. He is the author of more than 100 scientifical publications and technical patents.

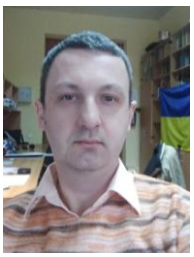

Oleksandr F. Kolomys, PhD in Physics and Mathematics. Senior Researcher at the Laboratory of Submicron Optical Spectroscopy, V. Lashkaryov Institute of Semiconductor Physics. Authored over 130 publications, 3 patents, 3 chapters of text-books. The area of his scientific interests includes Raman and luminescent microanalysis of light emitting properties, structure, composition, electronic and phonon excitations in solids, physical and chemical properties of semiconductors, chemicals and nanostructures for modern micro-, nano- and optoelectronics with submicron spatial resolution.

Olexander I. Bykov, PhD in Engineering. Leading Researcher at the I. Frantsevych Institute for Problems of Materials Science, NAS of Ukraine. Author of more than 200 publications. His research interests include solid state physics, XRD.

Volodymyr O. Yukhymchuk, Doctor of Sciences, Professor, Head of Department of Optics and Spectroscopy, V. Lashkaryov Institute of Semiconductor Physics. The area of scientific interests includes physics of semiconductors, solid state physics, optics, materials diagnostics, nano-structures, Raman spectroscopy, SERS.

Maksym M. Zahornyi, PhD in Physical and Organic Chemistry, Senior Researcher at the I. Frantsevych Institute for Problems of Materials Science. Author of more than 50 publications. His research interests include: polymeric chemistry, functional materials.

Kostiantyn A. Korotkov, Lead Engineer at the I. Frantsevych Institute for Problems of Materials Science. Author of more than 4 publications. His research interests include solid state physics, physics properties and technology of thin films.

Valentyna M. Karavaieva, Chief Technologist at the I. Frantsevych Institute for Problems of Materials Science, NAS of Ukraine. Author of more than 50 publications.
Her research interests include solid state physics, physics properties and technology of thin films

Sergiy F. Korychev, Researcher at the I. Frantsevych Institute for Problems of Materials Science, NAS of Ukraine. Author of more than 15 publications.
His research interests include solid state physics, XRD.

Arsenii I. Ievtushenko, PhD in Physics and Mathematics, Head of Department of Physics and Technology of Photoelectronic and Magnetoactive Materials at the I. Frantsevych Institute for Problems of Materials Science, NAS of Ukraine. Author of more than 170 publications.
His research interests include solid state physics, functional materials

Властивості нанорозмірних плівок ZnO:Ho, нанесених вибуховим випаровуванням

А.М. Касумов, В.В. Стрельчук, О.Ф. Коломис, О.І. Биков, В.О. Юхимчук, М.М. Загорний, К.А. Коротков, В.М. Караваєва, С.Ф. Коричев, А.І. Євтушенко

Анотація. Досліджено властивості нанорозмірних плівок ZnO:Ho, нанесених вибуховим випаровуванням. Метою даної роботи є вивчення впливу великої швидкості осадження на характеристики даного оксиду, які використовуються для процесу фотокаталізу, такі як морфологія і структура, електричні та оптичні властивості, час життя носіїв заряду. Вибухове осадження плівок зумовлює новизну даної роботи стосовно більшості попередніх досліджень нанорозмірних фотокаталізаторів ZnO:Ho, де було використано рівноважні методи їх синтезу. Методами скануючої електронної мікроскопії, рентгеноструктурного аналізу, фотолюмінесценції та раманівського розсіяння показано, що при вибуховому нанесенні плівок ZnO:Ho зі збільшенням вмісту лігатури спостерігається аморфізація їх структури і зміна морфології, які пов'язані з хаотичним вбудовуванням атомів Ho в кристалічну ґратку ZnO, а також перевищенням іонного радіуса Ho^{3+} над Zn^{2+}. Аморфізація супроводжується зсувом краю поглинання ZnO у довгохвильову (синю) область спектра, зменшенням ширини його забороненої зони, зростанням питомого опору та часу життя носіїв заряду. Всі ці зміни є сприятливими для процесу фотокаталізу за участю наноструктур на основі ZnO:Ho.

Ключові слова: плівки, оксид цинку, гольмій, фотокаталізатор, вибухове випаровування.